Controllable Laser Ion Acceleration

Controllable Laser Ion Acceleration

S Kawata[1], D Kamiyama[1], Y Ohtake[1], M Takano[1], D Barada[1], Q Kong[2], P X Wang[2], Y J Gu[3], W M Wang[4,5], J Limpouch[6], A Andreev[7,8], S V Bulanov[9,10], Z M Sheng[11], O Klimo[6], J Psikal[6], Y Y Ma[12], X F Li[2], and Q S Yu[2]

[1]Graduate School of Engineering, Utsunomiya University, Utsunomiya, Japan.
[2]Institute of Modern Physics, Fudan University, Shanghai, China
[3]ELI Beamlines, Institute of Physics, Prague, Czech Republic
[4]Institute of Physics, CAS, Beijing, China
[5]Forschungszentrum Juelich GmbH, Juelich, Germany
[6]Czech Technical University in Prague, Prague, Czech Republic
[7]Max-Born-Institut, Berlin, Germany
[8]Vavilov State Optical Institute, St.-Petersburg, Russia
[9]Japan Atomic Energy Research Institute, Kyoto, Japan
[10]A M Prokhorov General Physics Institute, Moscow, Russia
[11]Key Laboratory for Laser Plasmas and Department of Physics and Astronomy, Shanghai Jiao Tong University, Shanghai, China
[12]Department of Physics, National University of Defense Technology, Changsha, China

E-mail: kwt@cc.utsunomiya-u.ac.jp

Abstract. In this paper a future laser ion accelerator is discussed to make the laser-based ion accelerator compact and controllable. Especially a collimation device is focused in this paper. The future laser ion accelerator should have an ion source, ion collimators, ion beam bunchers, and ion post acceleration devices [Laser Therapy **22**, 103(2013)]: the ion particle energy and the ion energy spectrum are controlled to meet requirements for a future compact laser ion accelerator for ion cancer therapy or for other purposes. The energy efficiency from the laser to ions is improved by using a solid target with a fine sub-wavelength structure or a near-critical density gas plasma. The ion beam collimation is performed by holes behind the solid target or a multi-layered solid target. The control of the ion energy spectrum and the ion particle energy, and the ion beam bunching would be successfully realized by a multi-stage laser-target interaction.

1. Introduction

Intense short pulse lasers have been widely used for many purposes, including material processing, laser plasma interaction, radiation generation, particle acceleration, etc. Proton or carbon beams are effective to kill cancer cells, and the ion-beam cancer therapy has contributed to cure patients. Conventional ion accelerators are huge and expensive. Recently laser-based ion beam generation has been actively studied to generate ion beams [1-6]. However, the laser-based ion acceleration has met a lack of the controllability.

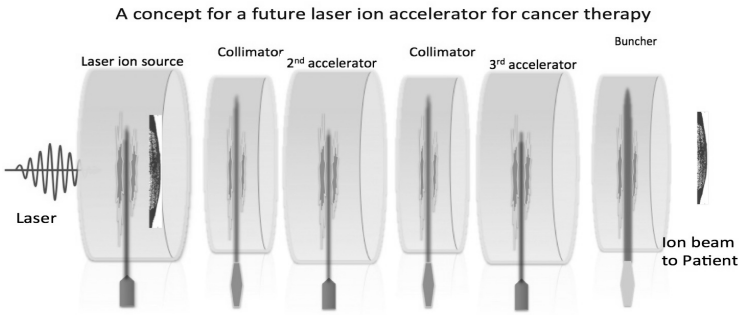

Figure 1. Concept of an example future laser ion accelerator. An intense laser illuminates a target, and a proton beam is generated at the ion source. For ion cancer therapy as an example application, the proton energy must be 200-400 MeV to kill tumor inside a human body. Further post-acceleration devices would be required to enhance the proton energy to achieve 200-4000MeV of proton energy and also to control the ion energy spectrum. In addition, ion collimators / focusing devices would be also needed to suppress the ion beam divergence. In order to compress the ion beam longitudinally, a beam buncher may be required.

In this paper first we briefly introduce a concept of a controllable laser ion acceleration system, which has been recently proposed (see Fig. 1) [6]. Then the ion beam collimation is focused in this paper [7, 8] in the laser plasma interaction, in which a thin-foil structured target is employed; the structured thin foil target (see Fig. 2) has holes behind the target to generate the transverse electric field, which contributes to the reduction of the ion beam transverse velocity toward the ion beam collimation. The structured target, which has the holes behind the target, was proposed in Refs. 7 and 8 to produce the collimated ion beam at the ion source [6]. However, the laser-produced ion beam tends to expand in the transverse direction, as well as in the longitudinal direction, during the ion beam propagation after its generation at the ion source. In this paper the structured thin-foil target with the holes at the target rear side [7, 8] is employed to collimate the laser pre-produced ion beam. The 2.5-dimensional particle-in-cell simulations are performed to investigate the ion beam collimation.

2. Controllable laser ion acceleration

Figure 1 shows a concept proposed for a future laser ion accelerator [6]. In an intense laser interaction with a target, first ions are generated at an ion source device. The protons are accelerated by the strong electric field produced at the target by the laser-target interaction, in which the target electrons are

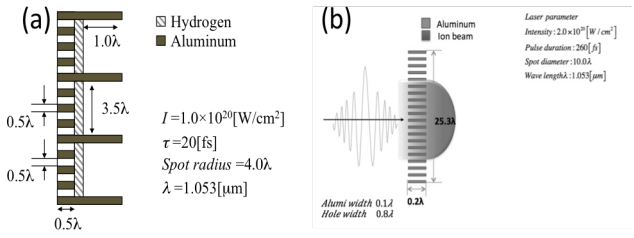

Figure 2. (a) An example laser ion source, which has fine holes at the laser side (left) to enhance the laser energy absorption and wider holes behind the target to collimate the proton beam at the ion source. (b) An example ion beam buncher: the TNSA (target normal sheath acceleration) field is used to compress the longitude proton beam length in this specific case.

expelled quickly and the target becomes a plasma. The high-energy electrons move around the target and the target ions stay at rest during a short period of ~fs. Between the ions and the high-energy electrons, a strong electric field is generated and accelerates protons gradually. In the ion-source stage the ion beam tends to have a lower particle energy, a broad energy spectrum and a transverse divergence. For ion cancer therapy as an example application, the ion energy spectrum should be controlled and the ion energy should be about 250-400MeV to deposit the ion energy in cancer cells inside human body.

Therefore, the laser ion accelerator would need post-acceleration devices to enhance the ion energy by a solid target as shown in Fig. 2(a) or by a near-critical gas target [6], and collimators to suppress the ion divergence (see Fig. 3), as well as beam bunchers (see Fig. 2(b)) to compress the ion beam longitudinally. Depending on the requirements for the proton energy and the beam radius, the laser ion accelerator would be designed appropriately as shown in Fig. 1.

3. Robust collimation of laser produced ion beam

Figure 3 shows the collimation device and the simulation setup employed in this paper. The sub-wavelength fine structure at the thin foil itself increases the laser absorption ratio [9-12], and the larger holes at the target rear creates the transverse TNSA (target normal sheath acceleration) field to collimate the ion beam. The ion beam diameter of 10λ is smaller than the rear hole diameter of 19.7λ (the wall width in Figs. 3 and 4) to avoid the ion beam split [7, 8]. The pre-accelerated proton beam is shown in Figs. 5(a) and (d), and is introduced to the simulation box initially. The pre-accelerated proton beam has the divergence angle shown in Fig. 6(a) and the energy and spatial distributions in Figs. 5(a) and (d). The Gaussian laser intensity is 4.0×10^{19}W/cm^2, the laser spot size is 50λ and the laser pulse length is 100fs. Figure 4 shows the transverse collimation electric field at the target during the laser illumination. Figures 5(a)-(c) show the ion beam distributions at t=0fs, 300fs and 580fs without the collimation device, respectively. Figures 5(d)-(f) present the typical results with the collimation device at t=0fs, 300fs and 580fs, respectively. Figures 5(d)-(f) demonstrate that the collimation device is effective for the ion beam collimation. Figure 6 shows the ion beam divergence angle, and presents the clear collimation of the ion beam by the structured target.

We have investigated the robustness of the collimation device against the changes in the laser intensity, the laser illumination timing, the structured target wall length and the target wall width. The definitions for the target wall length and width are presented in Fig. 3. Figures 7(a)-(d) summarize the results for the parameter studies to find the robustness of the collimation device.

Figure 7(a) shows the relation between the ion beam divergence angle and the laser intensity. When the laser intensity is weak compared with the optimal laser intensity, the ion beam collimation field is

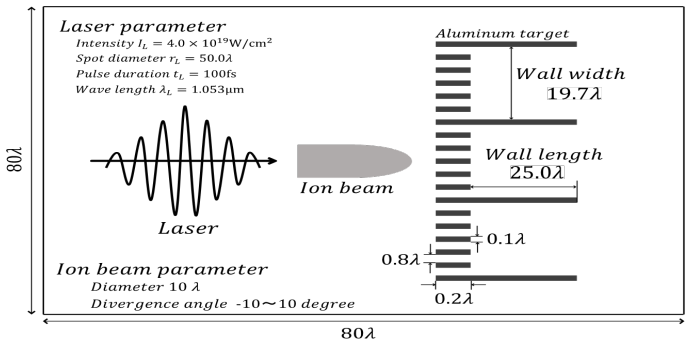

Figure 3. Structured thin-foil collimation device for ion beam. A pre-accelerated proton beam is introduced to the collimation device. The holes' walls create the transverse electric TNSA field to collimate the ion beam.

weak. On the other hand when the laser intensity is too high, the ion beam is over-focused. Figures 8 present the beam proton distributions and the proton divergence angle distributions for the laser intensity shown in the figure. The allowance of the laser intensity is rather wide as presented in Fig. 7(a). Figure 7(b) shows the relation between the ion beam divergence angle and the target wall width (see Fig. 1). For a specific laser intensity, when the wall width becomes narrow, the transverse collimation electric field becomes strong and so the collimation effect becomes too strong. When the wall width is too large, the electric field felt by the beam ions becomes small. Figures 8 shows typical example simulation results for the different target wall widths. In this paper the ion beam diameter is 10λ. Figures 7(b) and 9 show that the wall width should be the order of the beam diameter. Figure 7(c) shows the relation between the ion beam divergence angle and the target wall length (see Fig. 4). When the target wall length is too short, the time period, during which the beam protons feel the collimation transverse electric field, becomes short. So the collimation effect becomes weak for the short target wall length. When the target wall length becomes too long, a part of the long wall near the laser target interaction area in which the target has a fine structure has the collimation electric field. So the rest of the long target wall has no effect for the collimation, and the too-long wall does not degrade the collimation effect. Figures 10 present the typical simulation results in this case. Figure 7(d) presents the relation between the ion beam divergence angle and the laser timing. When the laser timing is too fast, just the head of the ion beam is collimated. When the laser timing is late, the tail of the ion beam is collimated. Figures 11 show the typical simulation results for the corresponding laser timing. The laser pulse length is 100fs in this paper, and the tolerable laser-timing shift is rather wide as shown in Fig. 7(d).

All the parameter study results are summarized in Figs. 7 and demonstrate that the collimation device of the structured target is rather robust against the changes in the laser parameter and the target parameter. The results presented in this paper show the viability of the laser-based collimation device for the collimation of the pre-accelerated ion beam, which may be produced by an intense-laser target interaction.

4. Conclusions

We have presented the robustness of the structured collimation target for the pre-accelerated ion beam against the laser and target parameter changes. In the collimation device the transverse electric field is employed to collimate the diverging beam ions and is generated by the intense-laser target interaction. The collimation device would be required for a long distance transportation of the ion beam pre-accelerated [6]. For actual applications of the ion beam, the ion beam should be transported in a long distance compared with the size of the laser target interaction area. The collimation device

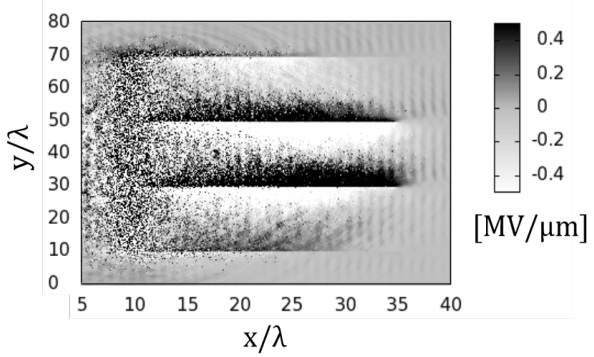

Figure 4. The transverse electric field. The Al structured target is illuminated by an intense laser. The fine structure absorbs the laser energy efficiently, and generates high-energy electrons. The TNSA transverse field is generated by the electrons collimates the proton beam.

proposed would be viable for a realistic long-distance ion beam transportation. For a practical laser-based ion beam accelerator [6], the multiple acceleration, collimation and bunching stages would be required to meet the application requirements for the ion beam quality, energy and intensity. The collimation device shown in this paper is one of the promising candidates for the pre-accelerated ion beam collimation.

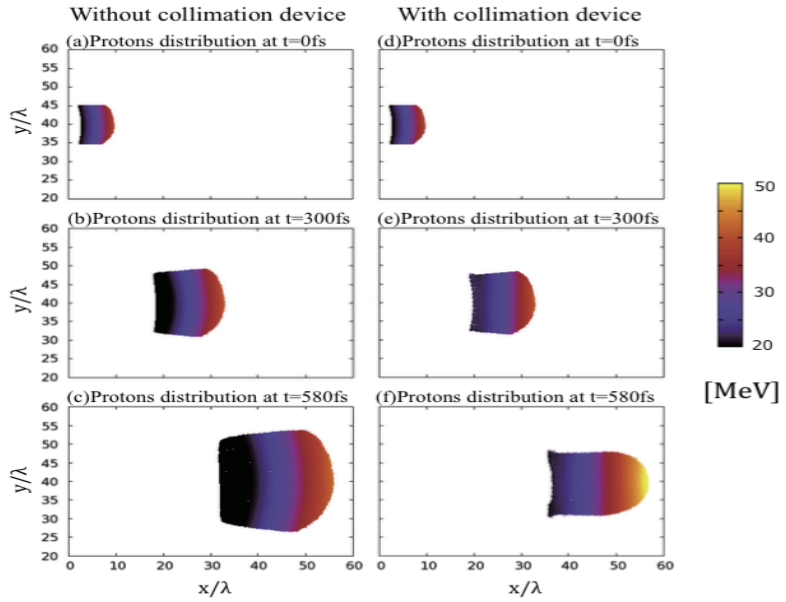

Figure 5. Spatial distributions of protons for the proton beam without the collimation device at (a)t =0fs, (b)t =300fs and (c)t=580fs, and for the proton beam with the collimation device at (d)t=0fs, (e)t=300fs and (f)t=580fs. The collimation device reduces the proton beam divergence successfully.

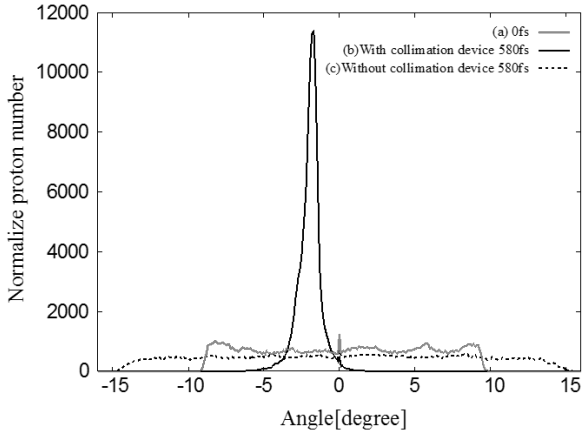

Figure 6. Divergence angle distributions for (a) the original proton beam (solid line), for (b) the proton beam without the collimation device (short-dotted line) and for (c) the proton beam with the collimation device (long-dotted line).

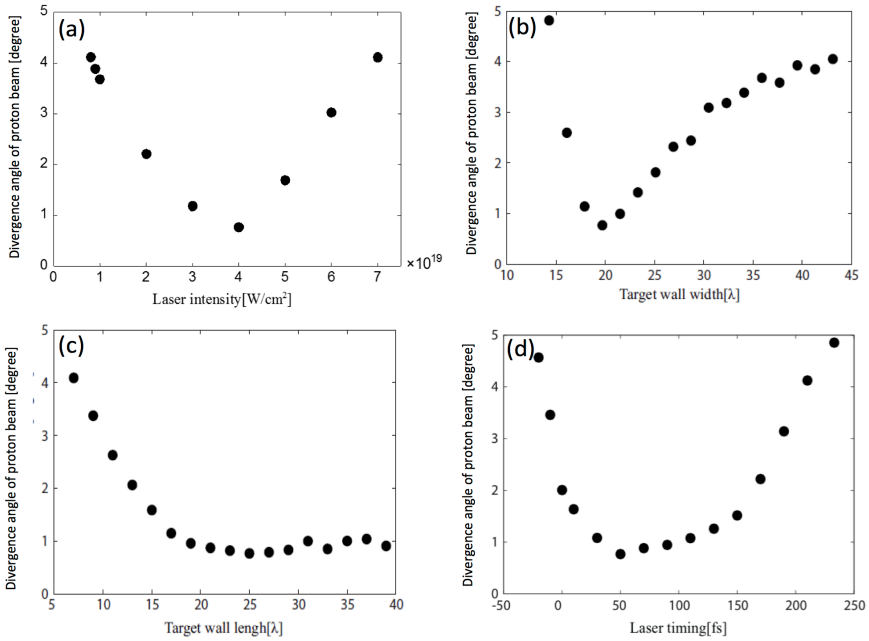

Figure 7. Divergence angle dependences of beam ions on (a) the laser intensity, (b) the target wall width, (c) the target wall length and (d) the laser timing. The collimation device shown in Fig. 3 is rather robust against the parameter changes in the laser parameters and the target structure.

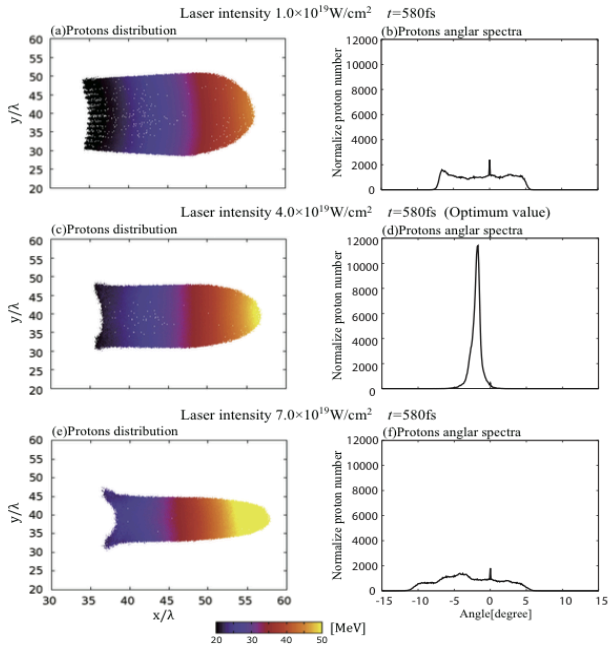

Figure 8. Distributions of the beam protons at the laser intensity of (a) $1.0\times10^{19}W/cm^2$, (c) $4.0\times10^{19}W/cm^2$ and (e) $7.0\times10^{19}W/cm^2$ at t=580fs. The corresponding distributions of the proton divergence angle are shown in (b), (d) and (f) at t=580fs.

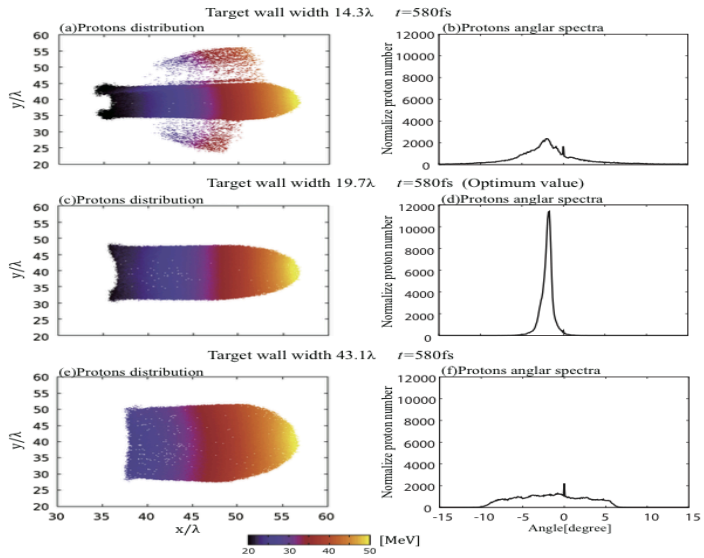

Figure 9. Distributions of the beam protons at the target wall width of (a) 14.3λ, (c) 19.7λ and (e) 43.1λ at t=580fs. The corresponding distributions of the proton divergence angle are shown in (b), (d) and (f) at t=580fs.

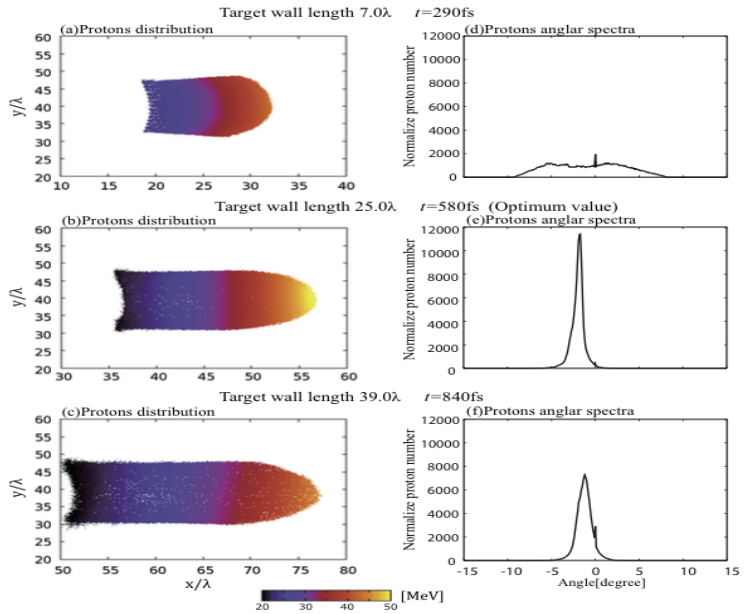

Figure 10. Distributions of the beam protons at the target wall length of (a) 7.0λ at t=290fs, (b)25.0λ at t=580fs and (c) 39.0λ at t=840fs. The corresponding distributions of the proton divergence angle are shown in (d), (e) and (f).

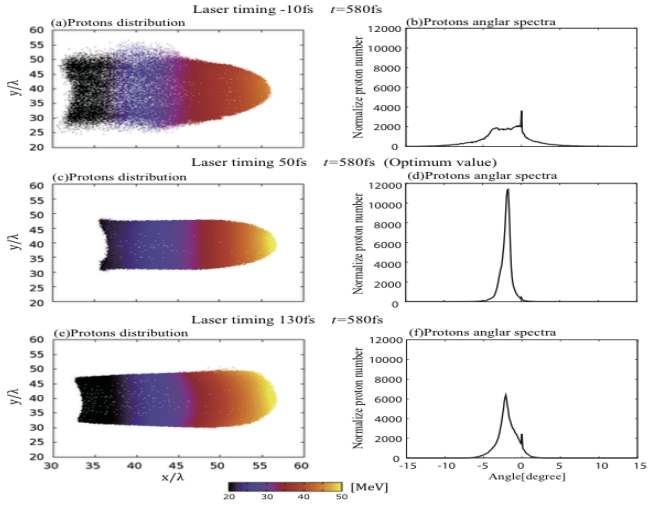

Figure 11. Distributions of the beam protons at the laser timing of (a) 10fs, (c) 50fs and (e) $130fs$ at t=580fs. The corresponding distributions of the proton divergence angle are shown in (b), (d) and (f) at t=580fs.

Acknowledgements
This work was partly supported by JSPS KAKENHI Grant Number 15K05359, MEXT, JSPS, the ASHULA project, ILE, Osaka University, CORE (Center for Optical Research and Education, Utsunomiya University, Japan), Fudan University and CDI (Creative Dept. of Innovation, CCRD, Utsunomiya University).

References

[1] Bulanov S V and Khoroshkov V S 2002 *Plasma Phys. Rep.* **28** 453
[2] Kaluza M, Schreiber J, Santala M I K, Tsakiris G D, Eidmann K, Meyer-ter-Vehn J and Witte K J 2004 *Phys. Rev. Lett.* **93** 045003
[3] Bulanov S V, Esirkepov T Zh, Califano F, Kato Y, Lisekina T V, Mima K, Naumova N M, Nishihara K, Pegorano F, Ruhl H, Sentoku Y and Ueshima Y 2000 *JETP Lett.* **71** 407
[4] Nakamura T and Kawata S 2003 *Phys. Rev. E* **67** 026403
[5] Nakamura T, Bulanov S V, Esirkepov T Z and Kando M 2010 *Phys. Rev. Lett.* **105** 135002
[6] Kawata S, Izumiyama T, Nagashima T, Takanao M, Barada D, Kong Q, Gu Y J, Wang P X, Ma Y Y and Wang W M 2013 *Laser Therapy* **22** 103
[7] Sonobe R, Kawata S, Miyazaki S, Nakamura M and Kikuchi T 2005 *Phys. of Plasmas* **12** 073104
[8] Nakamura M, Kawata S, Sonobe R, Kong Q, Miyazaki S, Onuma N and Kikuchi T 2007 *J. Appl. Phys.* **101** 113305
[9] Nodera Y, Kawata S, Onuma N, Limpouch J, Klimo O and Kikuchi T 2008 *Phys. Rev. E* **78** 046401
[10] Klimo O, Psikal J, Limpouch J, Proska J, Novotny F, Ceccotti T, Floquet V and Kawata S 2011 *New J. Phys.* **13** 053028
[11] Margarone D, Klimo O, et al. 2012 *Phys. Rev. Lett.* **109** 234801
[12] Dalui M, Wang W-M, et al. 2015 *Scientific Rep.* **5** 11930